Hydraulic fracture stage identification and size estimation using distributed strain and temperature sensing

Jaewon Saw[1], Linqing Luo[2], Julia Correa[2], Kenichi Soga[1], Xiaoyu Zhu[3], Jonathan Ajo-Franklin[3], Erich Kerr[4], Robert Bohn[4]*
[1]*University of California, Berkeley, CA, USA*
[2]*Lawrence Berkeley National Laboratory, Berkeley, CA, USA*
[3]*Rice University, Houston, TX, USA*
[4]*SM Energy Company, Denver, CO, USA*

Summary

We present a case study in which we analyze distributed strain sensing (DSS) and distributed temperature sensing (DTS) measurements from an actively fractured well, located in a field laboratory project investigating hydraulically fractured horizontal wells. By examining the spatio-temporal distribution of temperature-compensated strain, we identify distinct strain signatures corresponding to individual stages in the fracturing process and estimate fracture widths within the fracture zone. These findings demonstrate the effectiveness of distributed fiber optic sensing in monitoring the hydraulic fracturing process and assessing the resulting fracture system, as well as assisting future studies in the interpretation of strain signatures obtained from distributed strain and temperature sensing data.

Introduction

Researchers have noted the need for closely monitoring the various operations of the hydraulic fracturing process, including perforation, fracture fluid injection, proppant placement, fracture extension, flowback and production (Karrenbach et al., 2019; Molenaar et al., 2012; Webster et al., 2013; Zhu et al., 2023). Each operation has its own set of parameters, such as well-spacing, stage height, volume of injected fluids and proppants. When these parameters are optimized, the efficiency of oil and gas recovery may be significantly improved, and hence the pursuit for advanced monitoring methods forms an important part of the industry R&D (Bakku et al., 2014).

In recent years, there has been increased interest surrounding the application of distributed fiber optic sensing (DFOS) for such monitoring purposes. DFOS, a technology utilizing various types of optical backscattering reflectometry, transforms an optical fiber into an array of closely spaced sensing points. It provides a continuous profile of temperature, static strain, vibrations (dynamic strain), and other measurands of interest as a function of the distance along the sensing fiber (Hartog, 2017). Direct observation in the subsurface is inherently difficult (Fu et al., 2021), but DFOS gets around this difficulty by allowing sensor installation directly inside the well. By leveraging the distributed nature of the optical fiber, DFOS offers a solution for detecting localized events or changes that occur along the length of the fiber (Luo and Soga, 2018), which may be indicative of the state of the well itself as well as the surrounding environmental conditions.

A number of projects have demonstrated the potential of using DFOS technologies for gaining insights into hydraulic fracturing processes and the resulting fracture system, including fracture geometry, fracture conductivity, stage communication, perforation cluster fluid distribution, and fracture initiation points (e.g., Ramos Gurjao et al., 2022, Jin et al., 2020, Bakku et al., 2014; Leggett et al., 2023). As the industry currently stands, interpretation of DFOS data remains a major challenge faced by engineers and geoscientists, given the complexities associated with the field data (Ramos Gurjao et al., 2022; Pakhnotina et al., 2020). As the industry and research community head toward increased deployment of DFOS technologies in the backdrop of continued pursuit of multi-stage hydraulic fracturing in unconventional reservoirs, it becomes important to improve (1) our current scientific knowledge of how to process, analyze, and interpret the DFOS data as they relate to hydraulic fracturing; and (2) our fundamental understanding of subsurface processes that occur during hydraulic fracturing processes and operations. Detailed case studies can provide valuable insights into the complexities of hydraulic fracturing and offer opportunities to enhance future practices in utilizing DFOS for hydraulic fracturing applications.

In this work, we present our workflow and findings from analyzing distributed strain and temperature sensing measurements collected from a field laboratory project in Austin Chalk and Eagle Ford Shale Formations. We demonstrate that by detecting and identifying distinct tensile and compressive strain signals, it becomes possible to narrow down on smaller portions of the data and examine individual stages of the hydraulic fracturing process. This approach allows for a closer examination of relationships between different stages, enabling further investigation into phenomena such as fracture fluid communication, reopening of previously stimulated fractures, and the long-term residual effects that extend beyond a single stage and impact subsequent stages.

Methodology

For our study, we examine Distributed Strain Sensing (DSS) and Distributed Temperature Sensing (DTS) measurements collected from Well 3, which underwent active fracturing during our designated period of interest. While two other nearby wells – Wells 5 and 7 – were also subjected to fracturing during overlapping periods, our focus lies on the in-well measurements corresponding directly with the fracturing operations in Well 3.

Fracture stage identification and size estimation

The DSS and DTS readings are derived from Brillouin backscatter and Raman backscatter, which are optical phenomena used to measure strain and temperature along an optical fiber. Brillouin backscatter analyzes the frequency shift of the scattered light caused by acoustic waves to make the measurements, while Raman backscatter examines the wavelength changes of the scattered light resulting from molecular vibrations in the fiber (Hartog, 2017). In this study, we use a Brillouin optical-time domain reflectometry (BOTDR) system (Luo et al., 2019) for DSS and a Raman optical time-domain reflectometry (ROTDR) system (Silixa XT-DTS M) for DTS measurements. The temperature readings along the cable are used to compensate for the temperature effects from the strain measurements. Each system is deployed with its own data acquisition settings, shown in Table 1.

Table 1: Data acquisition settings and parameters

	DSS	DTS
Backscatter	Brillouin	Raman
Measurement type	Strain (with temperature effects)	Temperature
Measurement unit	microstrain	°C
Channel spacing	0.399 meters	0.5 m
Sampling frequency	1 sample / 20 minutes	1 sample / 30 seconds
Resolution	10-20 microstrain	0.01 °C

We first process the DSS readings by selecting the reference Brillouin frequency shift (BFS) at a time of no fracturing activity, established as the baseline from which strain values are later computed. We subtract this reference value from all BFS values and apply a moving average filter with a window size of 10 elements. We convert BFS to strain using Equation 1, which describes the dependence of BFS ν_B on temperature T and strain ε relative to reference temperature T_0 and reference strain ε_0:

$$\nu_B(T,\varepsilon) - \nu_B(T_0,\varepsilon_0) = C_T(T - T_0) + C_\varepsilon(\varepsilon - \varepsilon_0) \qquad (1)$$

C_T and C_ε are temperature and strain coefficients, which are dependent on multiple factors, including the optical fiber characteristics (e.g., core, cladding, jacket) and the wavelength of the pump laser (Bao et al., 2021). To convert the measured BFS into local temperature or strain changes, we employ approximations of $C_T \sim 1.025\ MHz/°C$ and $C_\varepsilon \sim 20\ \mu\varepsilon/MHz$.

We then process the DTS readings to strain by computing the relative changes in temperature from the previously established baseline, which are then converted to strain using the coefficient of $20.5\ \mu\varepsilon/\Delta°C$. Given that the DSS and DTS measurements occur at different spatial and temporal intervals, as indicated in Table 1, we align the readings through resampling and linear interpolation. Once the readings are aligned with consistent spatial and temporal sampling, we assume that the temperature at the DTS fiber reflects the temperature at the DSS fiber – given their relative proximity – and hence remove the temperature effects from strain.

The temperature-compensated strain measurements are visualized on a time-distance plot to observe the overall behavior of the stimulated reservoir and interpret spatial and temporal patterns in the data. Once individual stages of the hydraulic fracturing are identified, we interpret specific features of the strain signatures, such as fracture width growth and residual strain effects.

Results

We examine the spatio-temporal distribution of temperature-compensated strain (Figure 1 and Figure 3 center panel). The microstrain values are visually represented using a color scheme, with green indicating strain values close to zero, red representing positive tensile strain, and blue indicating negative compressive strain. To interpret this data, we also reference the well-side pressure (Figure 3, top panel) and perforation and production logs documented at the project site.

Figure 1: Temperature-compensated strain for Stage A

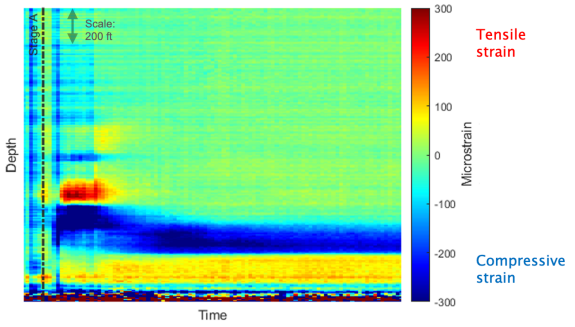

Initially, we observe the presence of strong strain signals, characterized by alternating bands of compressive and tensile strains spanning approximately 150 – 250 ft in width. Notably, we see a clear correlation with the borehole pressure, as indicated by the following observations: (1) the onset of these strain signals aligns with a rapid surge in pressure, (2) the highest strain magnitudes, represented by the dark red and blue colors in the plot, persist for a duration comparable to that of the peak pressure, and (3) the strain magnitudes diminish as the pressure rapidly declines. By cross-referencing the operation documentation, we confirm that the time stamps indicating the initiation of operations for each stage align with the pressure increase and the appearance of the strain signals, thus confirming the identification of stages in the hydraulic fracturing process.

Furthermore, we identify the fracture zones (indicated in red) and compressive zones (indicated in blue), as shown in Figure 4. Positive, tensile strains are observed in the fracture zones, where the opening of fractures leads to the stretching of the fiber that spans the fracture width. Negative strains are observed in the compressive reaction zones, where the fiber experiences compression, likely due to increased pressure resulting from the injection of fracking fluid.

With these observations, we also identify residual strain features. Initially, at the start of each stage, we observe the

highest levels of both tensile and compressive strains. Over time, the strength of the strain signals gradually diminishes, yet localized extrema remain discernible. Notably, these residual strains are spatially confined to the vicinity of the treated stage, aligning with the findings of Karrenbach et al. (2019) who reported similar observations. The detection of these residual strains prompts us to further explore similar features at other depths of the well, as indicated by grey arrows in Figure 4. Given that residual strains can extend into future stages, we consider the potential for fracture reconnection and the creation of multiple pathways for subsequent fractures. Notably, Leggett et al. (2023) conducted an analysis of low-frequency distributed acoustic sensing (LF-DAS) measurements collected from the same project site, interpreting the strain signals as indicators of fracture fluid communication with prior stages, which can lead to restimulation and reopening of previously stimulated fractures.

To analyze strain trends at specific depths, we compute the average strain within the fracture zone and its corresponding width for each stage. Multiplying these values provides an estimation of the fracture width. The resulting fracture width time series (Figure 3, bottom panel) reveals nonlinear patterns, with dotted circles indicating the non-linear increase and decline in fracture width during operations. This suggests that the injection of fracturing fluid induces strain and propagates fractures at the target depth. The fluid entering the fractures generates stress on the surrounding rock, causing an increase in strain and fracture width. As the fractures grow and expand, stress and strain are released, resulting in a decrease in strain and ultimately a decrease in fracture width. This consistent nonlinear pattern is observed for all stages depicted in the figure. The maximum fracture width is also observed for each stage, shown in Table 2.

Table 2: Maximum fracture width for an individual stage

Stage Number	Maximum Fracture Width (mm)
A	1.23
B	2.03
C	1.76
D	1.81

Figure 2: Average strain within the fracture zone for each stage, later used for computing fracture width within the fracture zone

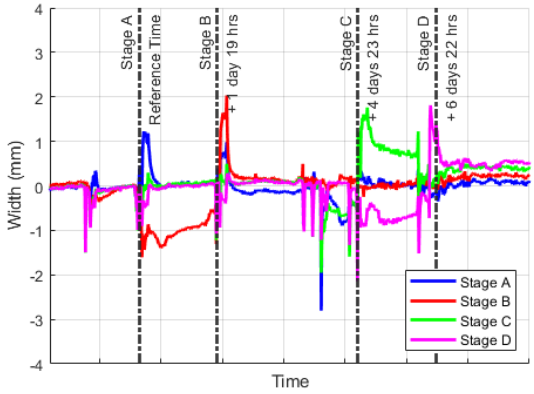

In summary, our analysis of temperature-compensated strain reveals clear correlations with well-side pressure, confirming the identification of individual stages in hydraulic fracturing. Positive tensile strains are observed in fracture zones, while negative strains occur in compressive zones. Residual strain features suggest potential fracture reconnection and the creation of multiple pathways for subsequent fractures. The examination of fracture width time series demonstrates nonlinear patterns, reflecting the influence of fracturing fluid injection on strain and fracture propagation. These findings highlight the valuable insights provided by distributed fiber optic sensing in understanding hydraulic fracturing dynamics.

Conclusions

We present our findings from analyzing the spatio-temporal distribution of temperature-compensated strain using distributed strain and temperature sensing measurements obtained from a hydraulically fractured horizontal well. The examination of distinct strain signatures in the data has provided valuable insights into the magnitude and duration of strain effects induced by the hydraulic fracturing processes. By identifying and studying individual stages within the hydraulic fracturing process, we have been able to gain further understanding of specific features related to fracture width growth and closure, residual strain effects, and fracture connectivity within the well. These findings underscore the effectiveness of distributed fiber optic sensing in monitoring the hydraulic fracturing process, assessing the resulting fracture system, and enabling future interpretations of strain signatures derived from distributed strain and temperature sensing data.

Future work may involve the development of an enhanced distributed strain sensing (DSS) system, particularly focusing on evaluating its performance in monitoring cross-well fracture events and improving strain resolution. Additionally, combining DSS and distributed temperature sensing (DTS) datasets, which require relatively shorter computational time, with other distributed fiber optic sensing technologies like low-frequency distributed acoustic sensing (LF-DAS) can provide complementary benefits. Furthermore, investigating the variation of strain around the circumference of the wellbore as a function of cable placement remains an area of interest, as determining the optimal cable location for capturing representative strain measurements is currently a source of uncertainty. By addressing these avenues of research, we can enhance the capabilities of distributed fiber optic sensing technologies and further advance our understanding of the complex dynamics involved in hydraulic fracturing processes.

Acknowledgements
Funding for LBNL was provided through the U.S. DOE, Assistant Secretary for Fossil Energy and Carbon Management, Office of Fossil Energy and Carbon Management, Resource Sustainability Program through NETL, under contract No. DE-AC02-05CH11231. We also thank SM Energy for providing the permission to publish this study.

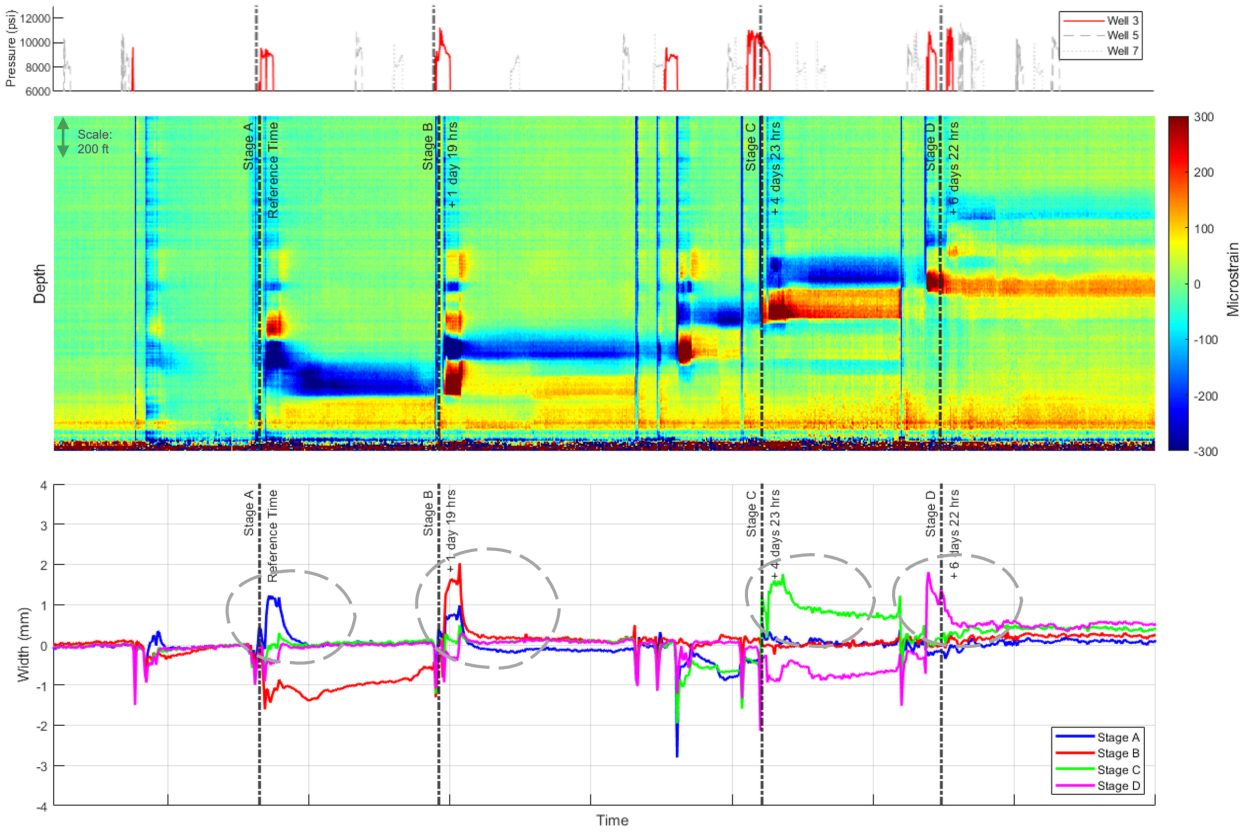

Figure 3: (Top) Well-side pressure distribution. (Center) Spatio-temporal distribution of temperature-compensated strain, with green, red, and blue indicating small magnitude, tensile, and compressive strains, respectively. The y-axis represents distance along the sensing cable, indicating depth in the well. Dotted vertical lines represent the timestamps of stage initiation. (Bottom) Time series of fracture widths corresponding to individual stages.

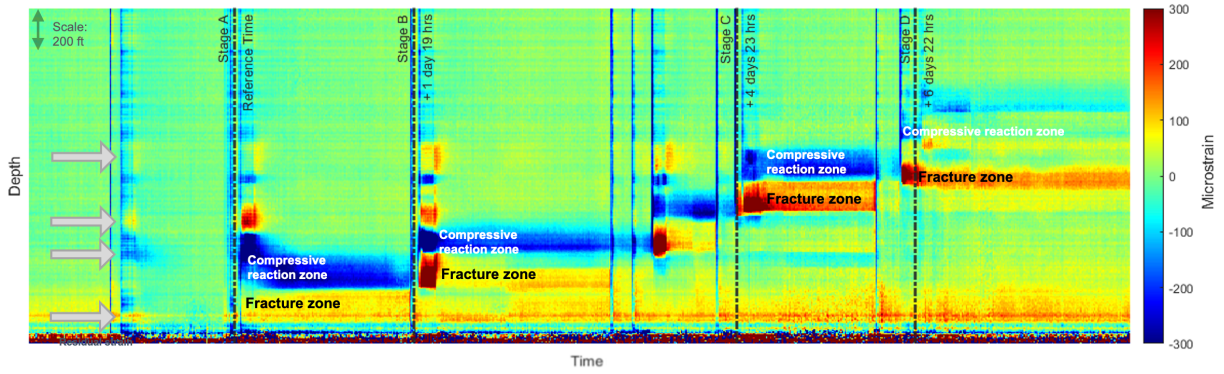

Figure 4: Labels indicate locations of fracture zones and compressive reaction zones. Grey arrows point to the depths along which we observe residual strain features from previous fracking operations.